# Ground and Excited State Resonance Raman Spectra of an Azacrown-Substituted $[(bpy)Re(CO)_3L]^+$ Complex: Characterization of Excited States, Determination of Structure and Bonding, and Observation of Metal Cation Release from the Azacrown

**Jared D. Lewis,[†] Ian P. Clark,[‡] and John N. Moore*[,†]**

*Department of Chemistry, The University of York, Heslington, York YO10 5DD, U.K. and Central Laser Facility, CCLRC Rutherford Appleton Laboratory, Chilton, Didcot, Oxfordshire OX11 0QX, U.K.*

*Received: August 28, 2006; In Final Form: October 10, 2006*

A $[(bpy)Re(CO)_3L]^+$ complex (bpy = 2,2′-bipyridine) in which L contains a phenyl-azacrown ether that is attached to Re via an amidopyridyl linking group has been studied by steady state and nanosecond time-resolved resonance Raman spectroscopy. Vibrational band assignments have been aided by studies of model complexes in which a similar electron-donating dimethylamino group replaces the azacrown or in which an electron-donor group is absent, and by density functional theory calculations. The ground state resonance Raman spectra show $\nu$(bpy) and $\nu$(CO) bands of the $(bpy)Re(CO)_3$ group when excitation is exclusively in resonance with the Re → bpy metal-to-ligand charge-transfer (MLCT) transition, whereas L ligand bands are dominant when it is in resonance with the strong intra-ligand charge-transfer (ILCT) transition present for L ligands with electron-donor groups. Transient resonance Raman (RR) spectra obtained on single color (385 nm) pulsed excitation of the complexes in which an electron-donor group is absent show $bpy^{\bullet-}$ bands of the MLCT excited state, whereas those of the complexes with electron-donor groups show both $bpy^{\bullet-}$ bands and a down-shifted $\nu$(CO) band that together are characteristic of an L-to-bpy ligand-to-ligand charge-transfer (LLCT) excited state. Samples in which a metal cation ($Li^+$, $Na^+$, $Ca^{2+}$, $Ba^{2+}$) is bound to the azacrown in the ground state show bands from both excited states, consistent with a mechanism in which the LLCT state forms after metal cation release from the MLCT state. Nanosecond time-resolved RR spectra from two-color (355 nm pump, 500 nm probe) experiments on the electron-donor systems show L-ligand bands characteristic of the LLCT state; the same bands are observed from samples in which a metal cation is bound to the azacrown in the ground state, and their time dependence is consistent with the proposed mechanism in which the rate constant for ion release in the MLCT state depends on the identity of the metal cation.

## Introduction

There has been significant interest in synthesizing and studying systems that can act as molecular switches[1] including light-controlled ion switches in which photoexcitation results in the release of a bound metal cation into solution.[2−10] "Single shot" systems for the light-controlled release of metal cations such as $Ca^{2+}$ are well developed, typically acting via an irreversible change, such as covalent bond cleavage, and they have enabled the effects to be studied in vivo with precise spatial and temporal specificity.[2−4] We have been studying light-controlled ion switches that operate by different mechanisms and in which the metal cation release is reversible.[5] Recently, we have been studying Re-coordinated azacrown ether systems that can produce light-induced pulses of $Li^+$, $Na^+$, $Ca^{2+}$, or $Ba^{2+}$ in solution due to rapid ion release in the excited state followed by slower thermal rebinding after relaxation to the ground state.[6,7]

Among the many types of organic and organometallic molecular switches that have been reported, $[(bpy)Re(CO)_3L]^+$ and related complexes have attracted interest because of their excited state electron and energy transfer reactions,[11,12] and they are increasingly being incorporated as chromophoric subunits within supramolecular devices.[13,14] The $[(bpy)Re(CO)_3L]^+$ complex **1** (shown below), which includes an amidopyridyl L ligand that terminates in an azacrown ether that can bind a metal cation ($M^{n+}$) to form **1**-$M^{n+}$, was originally reported in 1991 by MacQueen and Schanze.[15] They reported nanosecond time-resolved emission measurements and proposed a novel mechanism in which ion release occurs in the excited state of **1**-$M^{n+}$, limiting its effectiveness as a metal cation sensor. Their studies have prompted us to explore the potential of **1** as a light-controlled ion switch, and our recent picosecond and nanosecond time-resolved UV−visible absorption (TRVIS) studies have enabled us to observe the excited states and the reversible ion release-and-recapture cycles of **1**-$M^{n+}$ directly,[7,16] substantiating and extending the photochemical mechanisms that were originally proposed.[15]

For **1** without a metal cation bound (Scheme 1), excitation to the d$\pi$(Re) → $\pi$*(bpy) metal-to-ligand charge-transfer (MLCT) state is followed by intramolecular electron transfer from the azacrown nitrogen donor to the $Re^{II}$ center to create a ligand-to-ligand charge-transfer (LLCT) state in 0.5 ns ($k_{FET}^{-1}$), and back electron transfer from $bpy^{\bullet-}$ to $azacrown^{\bullet+}$ then regenerates the ground state in 19 ns ($k_{BET}^{-1}$).[15,16] For **1**-$M^{n+}$ where $M^{n+}$ = $Li^+$, $Na^+$, $Ca^{2+}$, or $Ba^{2+}$ (Scheme 2), excitation to the MLCT(on) state (i.e., with the metal cation bound) results in ion release to form the MLCT(off) state on a time scale of

[†] The University of York.
[‡] CCLRC Rutherford Appleton Laboratory.

10.1021/jp065563x CCC: $37.00 
Published on Web 12/14/2006

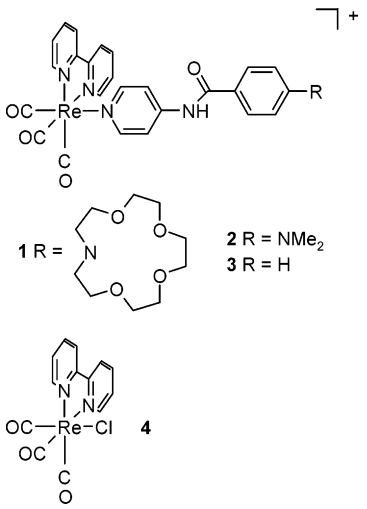


ca. 5−100 ns (dependent on the identity of $M^{n+}$), followed by intramolecular electron transfer to form the LLCT state, back electron transfer to regenerate the ground state with the metal cation out of the azacrown, and finally by metal cation rebinding from bulk solution on a time scale of ca. 0.1 $\mu$s − 1 ms (dependent on the identity of $M^{n+}$ and other sample conditions) to re-establish the starting thermal equilibrium.[7,16]

Our time-resolved UV−visible absorption studies provided clear kinetic information on the MLCT and LLCT excited states of **1**, and the distinct lifetimes enabled their TRVIS spectra to be observed distinctly despite their broad, overlapping features.[16] However, the situation was more complicated for **1**-$M^{n+}$ because the TRVIS spectra at ca. 10−50 ns were observed to depend on the identity of the metal cation:[7] the $Li^+$ and $Na^+$ samples gave characteristic LLCT state spectra that we attributed to fast ion release ($k^*_{off}{}^{-1} = 8$ and 6 ns, respectively) followed by fast forward electron transfer, whereas the $Ca^{2+}$ and $Ba^{2+}$ samples gave characteristic MLCT state spectra that we attributed to slower ion release ($k^*_{off}{}^{-1} = 90$ and 40 ns, respectively) being the slowest process and hence the rate-determining step in the excited state decay mechanism. In the absence of distinct TRVIS marker bands for the three excited states, we obtained these rate constants for ion release by fitting the transient absorption kinetics at 500 nm, where all three excited states contribute, to a kinetic model based on Scheme 2.[7] Our studies showed that the rate constants for $Li^+$, $Na^+$, $Ca^{2+}$, and $Ba^{2+}$ release in the excited state give the same variation with metal cation as those for ion release in the ground state, although they are higher in value, and that the rate constants for ion release in the ground state are important in controlling the ground state binding constants.[7] The general variation of ground state binding constants of azacrown systems with metal cation has been rationalized through a combination of several effects.[17]

In the present study, we have used resonance Raman (RR) spectroscopy to study the excited states of **1** and **1**-$M^{n+}$. Our aim was to exploit the well-established advantages of vibrational spectroscopy to provide marker bands that characterize different species more distinctly than electronic bands along with giving detailed information on their structure and bonding.[18] Time-resolved RR spectroscopy, in particular, is well-suited for studying samples containing several species because high sensitivity and good selectivity can be obtained by tuning the probe laser into resonance with the TRVIS bands of the different species present at various times after excitation. This approach appeared to be particularly appropriate for studying samples of **1**-$M^{n+}$ because several states with overlapping absorption bands and similar lifetimes were implicated in the ion-release mechanism.

**SCHEME 1: Photochemical Mechanism for 1 and 2**

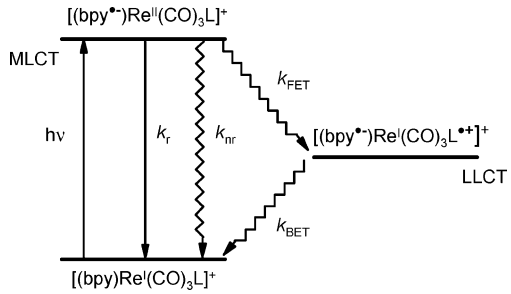


Hence, we report ground- and excited state RR spectra of **1**, **1**-$M^{n+}$, and three model complexes (shown above): **2**, in which the azacrown is replaced by a similar electron-donor dimethylamino group; **3**, in which the L ligand does not have a terminal electron-donor group; and **4**, in which the L ligand is replaced by a chloride ion. A combination of single-color transient resonance Raman ($TR^2$) and two-color time-resolved resonance Raman ($TR^3$) techniques has been used to record spectra that characterize the excited states, provide information on their structure and bonding, and enable light-controlled ion switching to be observed. In addition to providing further details on the photochemistry of this particular system, the study also illustrates more generally how the selectivity of RR spectroscopy may be used advantageously to study light-controlled ion-switching mechanisms.

## Experimental Section

Complexes **1**, **3**, and **4** were prepared according to literature methods[15,19] and characterized using $^1H$ NMR and electrospray ionization mass spectrometry, as reported previously.[7,16] Complex **2** was prepared similarly but using dimethylaminobenzoic acid as a starting material, and characterization details are given as Supporting Information. Samples were prepared in spectroscopic or HPLC grade acetonitrile (Aldrich) except for **1**-$M^{n+}$, where anhydrous acetontirile (Aldrich) was used as received and handled under nitrogen. $LiClO_4$ and $NaClO_4$ (Aldrich) were used as received; $Ca(ClO_4)_2$ and $Ba(ClO_4)_2$ (Aldrich) were dried under vacuum at 230 °C and stored under nitrogen. The rhenium complexes were used typically at ca. $(0.2-1.0) \times 10^{-3}$ mol $dm^{-3}$. The **1**-$M^{n+}$ samples were prepared at $[M^{n+}] \approx 0.1-0.8$ mol $dm^{-3}$, typically at ca. 50-fold in excess of the concentration given by the appropriate $K^{-1}$ value (where $K$ is the equilibrium constant for $M^{n+}$ binding to the azacrown)[7] to ensure that the samples contained ≤2% of **1** without a metal cation bound to the azacrown. Binding was confirmed by recording UV−visible absorption spectra.[7,20]

Steady state Raman spectra were recorded at York,[22] using a continuous-wave (CW) krypton ion laser (Coherent Innova 90) to provide 350.6 or 406.7 nm excitation with a power of ca. 30 mW impinging on a sample held in a capped spinning cell. Scattered light was collected at 90° to the incident beam, dispersed by a double monochromator (Spex 1403), and detected with a liquid-nitrogen cooled charge-coupled device (CCD) detector controlled by AT1 software (Wright Instruments). Spectra were recorded with a resolution of ca. 20 $cm^{-1}$, with an accuracy of ca. ±5 $cm^{-1}$ (±1 pixel) and with integration times in the range of 60−900 s. UV−visible absorption spectra were recorded using a Hitachi U-3000 spectrophotometer.

$TR^2$ and $TR^3$ spectra were recorded at the Central Laser Facility of the Rutherford Appleton Laboratory.[23] For single-

**SCHEME 2: General Photochemical Mechanism for 1-$M^{n+}$**

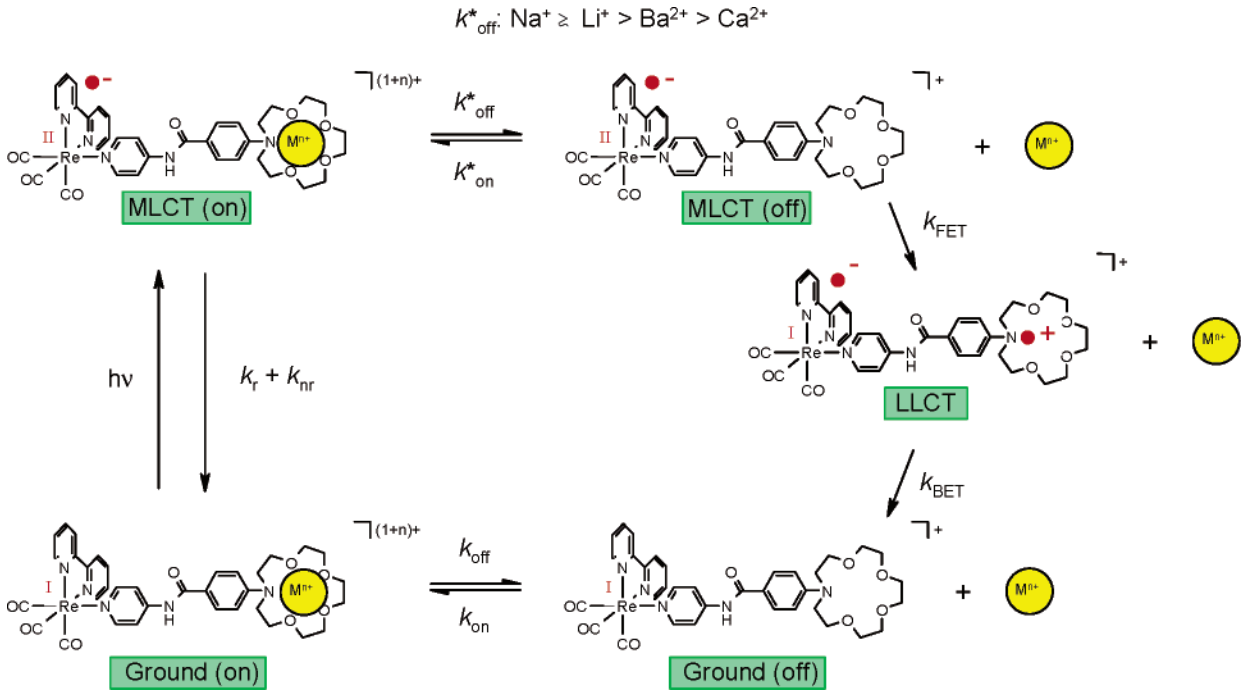


color TR[2] experiments, a dye laser (Lambda Physik FL3002; BIBUQ dye) pumped by a XeCl excimer laser (GSI Lumonics Pulsemaster 848) provided excitation at 385 nm (ca. 0.2−5.0 mJ energy; ca. 10 ns pulsewidth; 10 Hz repetition rate). For two-color TR[3] experiments, the third harmonic of a Nd:YAG laser (Continuum Powerlite 8000) provided a pump beam at 355 nm (ca. 1−5 mJ energy; ca. 7 ns; 10 Hz), the dye laser (LC 5000 dye) provided a probe beam at 500 nm (ca. 2−3 mJ energy), and signal-delay generators (Stanford Research Systems DG535) provided independent timing control between the two pulses. The samples were prepared at a concentration giving an absorbance of ca. 1 (in a 2 mm path length cell) at the excitation wavelength and were circulated, under continuous nitrogen purging, through a closed flow system with a 2 mm path length silica capillary cell that was mounted perpendicular to the entrance slit of a triple spectrometer (Spex Triplemate 1877). The samples were excited from below, and the scattered light was collected at 90° and detected by a liquid-nitrogen cooled CCD detector (Princeton Instruments Inc. LN/CCD-1024). Spectra were recorded with a resolution of ca. 10 $cm^{-1}$, an accuracy of ca. ±2 $cm^{-1}$ (± pixel), and integration times in the range of 200−600 s.

The Raman spectra were calibrated using solvent spectra (acetonitrile, dioxan, $d_{12}$-cyclohexane, toluene), recorded under identical conditions to those of the samples, and processed using Grams 386 software (Galactic Industries Corp.). Where necessary, a sloping baseline correction was made to correct spectra for the effect of sample emission.

Density functional theory (DFT) calculations were performed with the Gaussian 98 package[24] using the B3LYP functional and the 6-31G(d) basis set. The calculated vibrational frequencies were scaled by the recommended factor of 0.9613, and calculated spectra were created by applying a 5 $cm^{-1}$ full bandwidth Lorentzian function scaled to the relevant intensity of each calculated vibrational wavenumber.[22]

## Results and Discussion

**UV−Visible Spectra.** The UV−visible absorption spectra of **1**−**4** are shown in Figure 1. The spectra of **1** and **2** give intense bands at ca. 340 nm that are assigned to an intra-ligand charge-transfer (ILCT) transition localized at the L ligand, and bands at <300 nm that are assigned to $\pi \rightarrow \pi^*$ intra-ligand transitions localized at the L and bpy ligands.[15,16] Similar $\pi \rightarrow \pi^*$ bands at <300 nm also are present in the spectra of **3** and **4** but the intense ILCT band is absent due to the absence of an L ligand with a terminal electron-donor group, revealing a moderately intense band at ca. 350 and 370 nm, respectively, that is assigned to the Re → bpy MLCT transition.[15,16] A similar MLCT band at ca. 350 nm is expected for **1** and **2**, underlying the more intense ILCT band.

**Steady State RR Spectra.** Ground state RR spectra obtained on 350.6 nm CW excitation of **1**−**4** in acetonitrile are shown in Figure 2 along with a spectrum of **2** obtained on 406.7 nm CW excitation.

For **1** and **2**, 350.6 nm excitation is strongly in resonance with the ILCT transition (Figure 1) and the similar RR bands observed from these complexes (Figure 2 top) are assigned to vibrations centered on the L ligand. To obtain specific assignments, a Raman spectrum of the L ligand of **2** (L**2**) was calculated using DFT with the B3LYP functional and 6-31G(d) basis set, which has been reported to give accurate vibrational frequencies for small donor−acceptor 1,4-disubstituted phenyl systems of similar structure to L**2**.[25] The absence of the (bpy)Re(CO)$_3$ group and the use of a dimethylamino group rather than an azacrown within L simplifies the calculations[26]

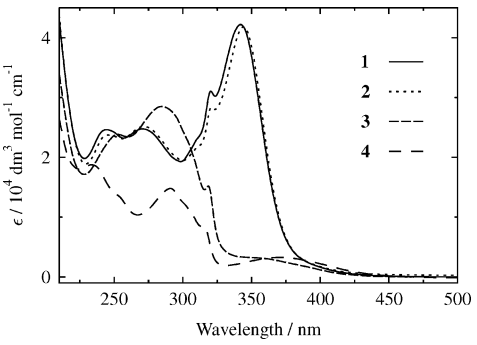


**Figure 1.** UV−visible absorption spectra of **1**−**4** in acetonitrile.

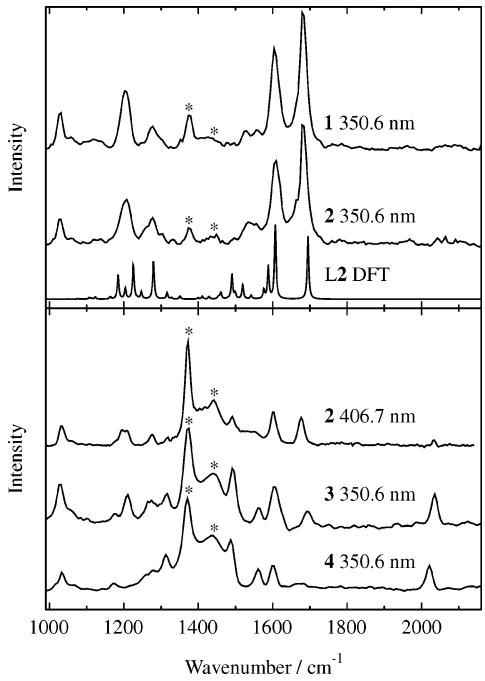


**Figure 2.** Top: steady state RR spectra of **1** and **2** in acetonitrile recorded with 350.6 nm CW excitation, along with the DFT calculated Raman spectrum of L**2**. Bottom: steady state RR spectra of **2** recorded with 406.7 nm CW excitation, and of **3** and **4** recorded with 350.6 nm CW excitation, all in acetonitrile. * indicates solvent band.

while giving results that our detailed studies have shown to model the IR and Raman spectra from related azacrown and Re-coordinated systems well.[22]

The calculated Raman spectrum of L**2** (Figure 2, top) gives a reasonably good agreement with the experimental RR spectra of complexes **1** and **2**. The calculated band positions for selected modes of L**2** are listed in Table 1, along with descriptions that indicate the major contributions derived from the calculated displacement vectors shown in Figure 3. Many of the calculated modes of L**2** involve significant motion of atoms throughout the molecule, indicating that there is coupling between the different parts of the ligand, and in-plane bending of the amide NH group contributes to several of the calculated modes. A number of the calculated modes of the amido ligand L**2** are comparable to those we have reported for the alkenyl and alkynyl analogues,[22] but the coupling between vibrations within the phenyl and pyridyl rings is generally weaker for L**2,** and it may result from incomplete conjugation resulting in a calculated twist between the rings (Figure 4) that contrasts the fully conjugated and essentially planar structures calculated for the alkene and alkyne systems.[27]

Table 1 lists the observed ground state RR bands of **1** and **2** along with their assignments based on the calculated ground-state modes of L**2**. The strong band of **1** and **2** at ca. 1680 $cm^{-1}$ can be assigned unambiguously to an amide I mode, which commonly gives a strong Raman band in this region and involves CO stretching and N−H in-plane bending,[28,29] as calculated here for L**2** at 1695 $cm^{-1}$ (Figure 3).[30] The strong RR band of **1** and **2** at ca. 1604 $cm^{-1}$ is broad, and three calculated modes may contribute to it: a shoulder at ca. 1620 $cm^{-1}$ is assigned to a band arising from a Wilson 8a vibration of the phenyl ring calculated at 1607 $cm^{-1}$ (Figure 3); the dominant peak at ca. 1604 $cm^{-1}$ is assigned to a band arising from a similar 8a vibration of the pyridyl ring calculated at 1588 $cm^{-1}$ (Figure 3); and a weaker band arising from N−H bending and a Wilson 8b vibration of the pyridyl ring (Figure 3) may contribute at ca. 1576 $cm^{-1}$.[31] The 8a vibration involves stretching along the axis of the substituents, and it commonly gives an intense band in the Raman spectra of compounds containing donor−acceptor 1,4-disbustituted rings.[25] Our calculations on L**2** indicate that the 8a vibration is strongly mixed with the Wilson 9a in-plane C−H bending vibration, as reported for related compounds.[22,25] There is also some coupling between the 8a/9a vibrations within the phenyl and pyridyl rings, but these modes are calculated to be more localized on a specific ring for L**2** than for the alkenyl and alkynyl analogues,[22] as discussed above. The moderately intense band of **1** and **2** at 1278 $cm^{-1}$ is assigned to an amide III mode, which commonly gives a strong Raman band in this region and involves C−N stretching and N−H bending.[28,29] In the case of L**2**, it is calculated to occur at 1279 $cm^{-1}$ and to be coupled strongly to a pyridyl ring 18a vibration and more weakly to a phenyl ring 3 vibration (Figure 3). The strong band of **1** and **2** at ca. 1206 $cm^{-1}$ is broad, and two modes may contribute to it. A strong contribution is assigned to a 9a vibration of the pyridyl ring calculated at 1204 $cm^{-1}$ (Figure 3), and a weaker contribution is assigned to a similar 9a vibration of the phenyl ring calculated at 1184 $cm^{-1}$ (Figure 3); these two bands are observed as two peaks in the RR spectrum of **2** obtained on 406.7 nm excitation. The moderately strong band of **1** and **2** at 1030 $cm^{-1}$ is assigned to coupled 18a and 19a vibrations within the pyridyl ring calculated at 1051 $cm^{-1}$. In summary, the RR bands of **1** and **2** are assigned to L-ligand modes that, apart from the amide I mode, generally involve ring vibrations that are symmetric along the axis of the substituents; the stronger bands arise from modes involving a significant contribution from the pyridyl ring.

For **3** and **4**, 350.6 nm excitation is in resonance with the MLCT transition (Figure 1), and the similar RR bands observed from these complexes (Figure 2, bottom) are assigned principally to vibrations centered on the $Re(CO)_3(bpy)$ group. For **4**, which has a chloride ion instead of an L ligand, the RR bands at <1700 $cm^{-1}$ have been assigned to bpy modes,[32] and the band at 2024 $cm^{-1}$ to the totally symmetric A′(1) $\nu(CO)_{Re}$ mode;[32,33] the other two $\nu(CO)_{Re}$ modes usually give strong IR bands but vanishingly weak RR bands in $Re(CO)_3(bpy)$ complexes,[33] and they are not observed in the RR spectra reported here. Table 1 lists the observed ground state RR bands of **3** and **4**, along with their assignments: the bpy modes are assigned in accordance with a reported vibrational analysis of the bpy ligand in $Ru(bpy)_3^{2+}$,[34] and two bands observed from **3** but not **4** are assigned to L ligand modes discussed above with their observation being attributable to preresonance enhancement from the $\pi \rightarrow \pi^*$ transition at shorter wavelength (Figure 1).

The RR spectrum of **2** obtained on excitation at 406.7 nm, to the red of the intense ILCT band and within the tail of the MLCT absorption band (Figure 1), gives a band pattern that approaches that of **3** obtained on excitation at 350.6 nm (Figure 2, bottom). Accordingly, the bands in this spectrum of **2** are assigned to bpy modes and the A′(1) $\nu(CO)_{Re}$ mode, as well as to some of the L-centered modes discussed above (Table 1).

**Single-Color TR² Spectra.** Single-color $TR^2$ spectra were recorded on pulsed excitation at 385 nm with each laser pulse providing both pumping and probing photons. Excited state bands were identified by an increase in their intensity relative to ground state bands as the laser pulse energy was increased, and they are seen most readily as positive bands in difference spectra obtained by the scaled subtraction of a RR spectrum at low pulse energy from one at high pulse energy, as shown in Figure 5 and Figure 6 (left).

**TABLE 1: Observed RR Band Positions ($cm^{-1}$) for Ground and Excited States of 1−4 in Acetonitrile, [a−d] Calculated Positions for Ground State L2, and Assignments**

| **1** | | | **1**-$M^{n+}$ | **2** | | | | **3** | | **4** | | L**2** | assignment | |
|---|---|---|---|---|---|---|---|---|---|---|---|---|---|---|
| $CW^a$ ground | $TR^2$ LLCT | $TR^3$ LLCT | $TR^2$ MLCT[i] | $CW^a$ ground | $CW^b$ ground | $TR^2$ LLCT | $TR^3$ LLCT | $CW^a$ ground | $TR^2$ MLCT | $CW^a$ ground | $TR^2$ MLCT | DFT ground | L-centered[e] | Re-centered[f] |
| | 2012 | | 2080 | | 2035 | 2012 | | 2035 | | 2024 | | | | $\nu(CO)_{Re}$ |
| 1683 | | | | 1679 | 1679 | | | 1692 | | | | 1695 | $\nu$(CO) + NH bend (amide I) | |
| 1620 sh[j] | 1514[g] | 1514 | | 1620 sh[j] | 1615 sh | 1514[g] | 1514 | | | | | 1607 | 8a/9a (ph) | |
| 1604[j] | | | | 1608[j] | | | | | | | | 1588 | 8a/9a (py) | |
| *j* | | | | *j* | | | | | | | | 1576 | NH bend + 8b/3 (py) | |
| | 1556 | | 1552 | | 1602[g] | 1556 | | 1604[i] | 1547 | 1601 | 1548 | | | $\nu_5$ (bpy) |
| | 1514[g] | | 1504 | | | 1514[g] | | 1563 | 1498 | 1563 | 1499 | | | $\nu_6$ (bpy) |
| 1558 | | | | 1558 | | | | | | | | 1542 | 8b/3 (ph) | |
| 1529 | | | | 1535 | | | | | | | | 1519 | 18a/19a (ph) + Me + $\nu$(ph-N) | |
| | | | 1486 | | 1495 | | | 1490 | 1478 sh | 1486 | 1479 sh | | | $\nu_7$ (bpy) |
| | 1420 | | 1422 | | *h* | 1420 | | *h* | 1421 | *h* | 1421 | | | $\nu_8$ (bpy) |
| | 1382 | | 1379 | | 1317 | | | 1314 | 1362 | 1314 | 1367 | | | $\nu_9$ (bpy) |
| 1278 | | | | 1278 | | | | | | | | 1279 | NH bend (amide III) + 18a (py) | |
| | 1280 | | 1279 | | 1277 | 1280 | | 1277 | 1274 | 1277 | 1279 | | | $\nu_{10}$ (bpy) |
| | 1221 | | 1215 | | | 1221 | | 1262 | 1213 | 1262 | 1216 | | | $\nu_{11}$ (bpy) |
| 1206[k] | | | | 1209[k] | 1209 | | | 1209 | | | | 1204 | 9a (py) | |
| *k* | | 1216 | 1168 | *k* | 1195 | | 1216 | | | | | 1184 | 9a (ph) | |
| | 1164 | | | | 1177 | 1164 | | 1173 | 1165 | 1173 | 1165 | | | $\nu_{12}$ (bpy) |
| | 1099 | | | | | 1099 | | | | | | | | $\nu_{13}$ (bpy) |
| 1060 | | 1022 | | 1060 | | | 1022 | | | | | 1075 | 18b (py) + 18a (ph) + NH bend | |
| | *l* | | 1019 | | 1031[g] | *l* | | 1031[g] | 1010 | 1031 | 1015 | | | $\nu_{15}$ (bpy) |
| 1030 | | | | 1030 | | | | | | | | 1051 | 18a/19a (py) | |

[a] CW 350.6 nm excitation. [b]CW 406.7 nm excitation. [c]$TR^2$ pulsed 385 nm excitation. [d]$TR^3$ pulsed 355 nm pump and 500 nm probe. [e]Assigned motions given in order of decreasing contribution based on calculations on L**2**, with ph = phenyl, py = pyridyl, and numbers indicating Wilson vibrations. [f] bpy = bipyridyl with mode numbers in accordance with ref 34. [g]L-centered and bpy-centered bands are near co-incident, and the observed feature may include a contribution from both. [h]Obscured by solvent band but reported[34] at 1450 $cm^{-1}$ for $Ru(bpy)_3^{2+}$. [i]Bands assigned to MLCT(on) state of **1**-$Ca^{2+}$ (see text). [j]The observed Raman band at ca. 1604 $cm^{-1}$ is broad and three calculated modes (as indicated) that give observable IR bands[31] may contribute (see text). [k]The observed Raman band at ca. 1200 $cm^{-1}$ is broad, and two calculated modes may contribute (see text). [l]Position uncertain because of overlying solvent or ground state band.

The excited state $TR^2$ spectra obtained on 385 nm excitation of **3** and **4** are similar to each other (Figure 5, bottom). Excitation at this wavelength pumps the MLCT transition and probes in resonance with the MLCT state band at ca. 370 nm that has been assigned to a transition localized on $bpy^{\bullet-}$.[7,16,19] The $TR^2$ spectrum of **4** has been reported previously and its bands have been assigned to modes of $bpy^{\bullet-}$[32], as given in Table 1,[34] in which we give equivalent assignments for **3**. Most of the excited-state bands are at a lower wavenumber than their ground state counterparts, showing downshifts of up to ca. 65 $cm^{-1}$ that are attributed to the occupation of a $\pi^*$ orbital in the MLCT state that weakens the bonds within the bpy rings. An exception is the band assigned to $\nu_9$, which involves a significant contribution from inter-ring bond stretching and shows an upshift of ca. 50 $cm^{-1}$ that has been attributed to an increase in the strength of this inter-ring bond in the MLCT state.[34] The close similarity of the $TR^2$ spectra of **3** and **4** indicates that the changes occurring on excitation are essentially localized on the $Re(bpy)(CO)_3$ group, and that the change from a chloride ion in **4** to an L ligand in **3** has little effect on the structure and bonding of the $bpy^{\bullet-}$ group in the MLCT state.

The excited state $TR^2$ spectra obtained on 385 nm excitation of **1** and **2** are similar to each other (Figure 5 top) with the strong negative features in these difference spectra arising from the bleaching of strong ground-state bands at ca. 1680 and 1604 $cm^{-1}$. Excitation at this wavelength pumps both the ILCT and MLCT transitions of **1** and **2**, but the absence of any TRVIS bands from the ILCT state in our picosecond and nanosecond TRVIS studies of **1** have shown that this state is very short lived.[16] Therefore, a 10 ns pulse at 385 nm probes in resonance with the ca. 370 nm TRVIS band of $bpy^{\bullet-}$ that is present for both MLCT and LLCT states (Scheme 1). The excited state bands in the $TR^2$ spectra of **1** and **2** are similar to those of **3** and **4**, and so most of the bands at $<1700$ $cm^{-1}$ are assigned to $bpy^{\bullet-}$, as given in Table 1. A significant difference is that **3** and **4** do not give a distinct excited state band in the 2000−2100 $cm^{-1}$ region, whereas **1** and **2** give a moderately strong band at 2012 $cm^{-1}$ that can be assigned to the A′(1) $\nu(CO)_{Re}$ mode of the LLCT state. The 23 $cm^{-1}$ downshift of this band from its ground state position is characteristic of weaker CO bonds that result from stronger back-bonding due to an increase in electron density at the $Re^I$ center, which is attached to a reduced bpy ligand in the LLCT state (Scheme 1). Similar downshifts have been reported for the equivalent IR band obtained on the electrochemical reduction of **4** to form $[(bpy^{\bullet-})Re(CO)_3Cl]$,[35] and on the photochemical formation of similar LLCT states of $Re(CO)_3$ systems with quite different diimine and L ligands.[14,36] The position of this $\nu(CO)_{Re}$ band provides conclusive evidence that these $TR^2$ spectra probe the LLCT state of **1** and **2**, and it is consistent with the 10 ns pulse

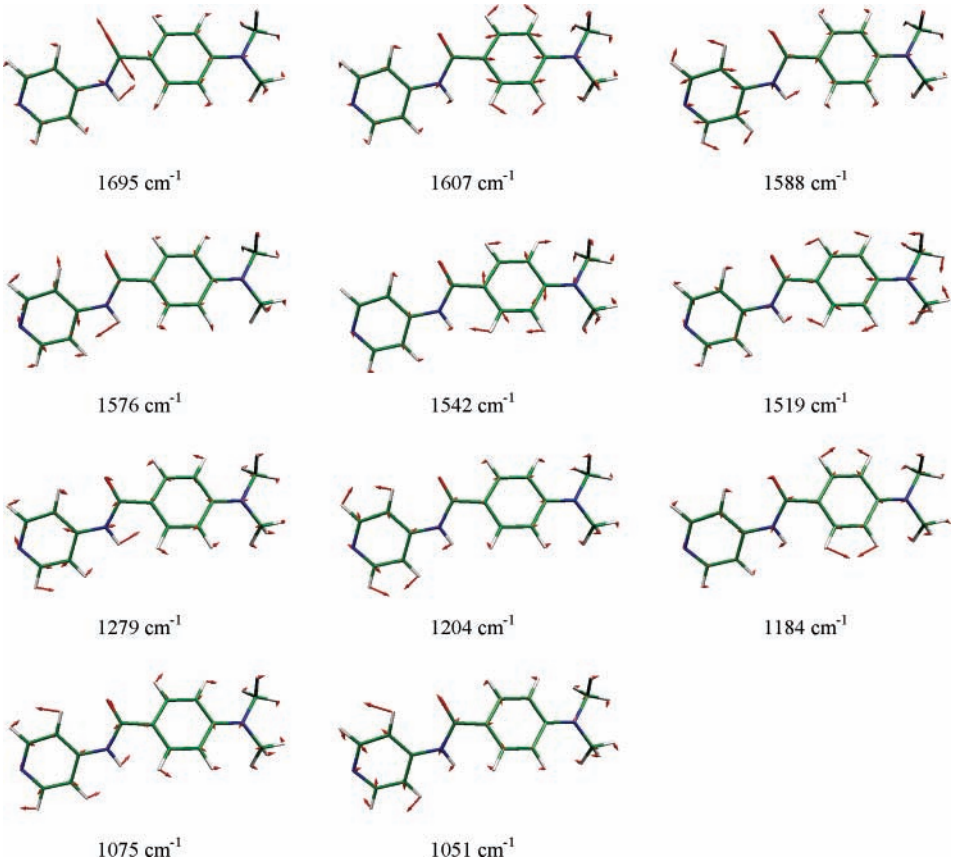


**Figure 3.** Selected calculated vibrational modes of L**2**.

giving preferential observation of the longer-lived LLCT state ($\tau$ = 19 ns) than the MLCT state ($\tau$ = 0.5 ns).[16] The close similarity in the $bpy^{\bullet-}$ bands of **1** and **2** in the LLCT state and **3** and **4** in the MLCT state (Figure 5) indicates that the structure and bonding within the reduced bpy ligand is similar in these two states, and the small differences in some of the band positions (Table 1) may arise from the different oxidation states of the attached Re atom (Scheme 1).[34,37] The $TR^2$ feature of **1** and **2** at 1514 $cm^{-1}$ can be assigned to an L-ligand centered band of the LLCT state, as discussed below in assigning the two-color $TR^3$ spectra, although it also may include a contribution from the $\nu_6$ $bpy^{\bullet-}$ band.

The excited state $TR^2$ spectra obtained on 385 nm excitation of **1**-$Li^+$, -$Na^+$, -$Ca^{2+}$ and -$Ba^{2+}$ are shown in Figure 6, along with those of **1** and **3** for comparison, with the 1975−2125 $cm^{-1}$ regions given directly (rather than as difference spectra) to show the excited state $\nu(CO)_{Re}$ bands together with the ground state bands present at ca. 2035 $cm^{-1}$ due to residual ground state sample. The spectra from **1**-$M^{n+}$ in the ca. 950−1750 $cm^{-1}$ region (Figure 6) are similar to those from **1**-**4** (Figure 5), and so most of the bands can be assigned to $bpy^{\bullet-}$. In addition, the **1**-$M^{n+}$ samples give bands at 1514 and 2012 $cm^{-1}$ that are observed from **1** and **2** but not from **3** and **4**, and have been assigned above to L-ligand and $\nu(CO)_{Re}$ modes, respectively, of the LLCT state. The observation of these two conclusive marker bands in a single-color $TR^2$ experiment indicates clearly that the LLCT state of **1** forms within ca. 10 ns on excitation

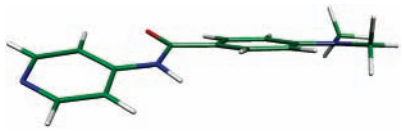

**Figure 4.** Calculated geometry of L**2**.[27]

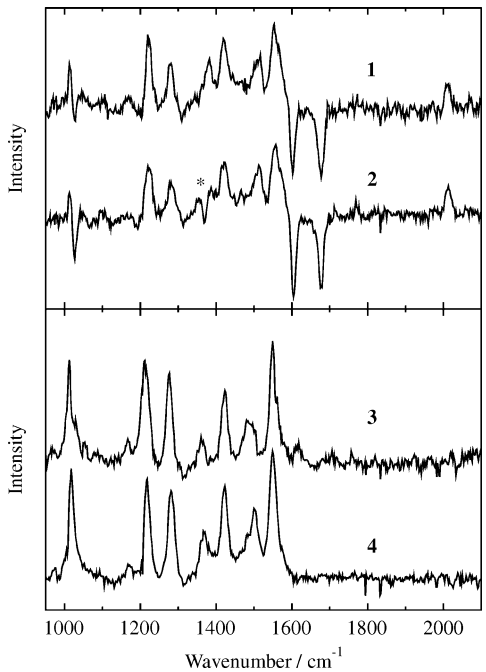


**Figure 5.** Excited state $TR^2$ spectra of (top) **1** and **2** and (bottom) **3** and **4** in acetonitrile recorded with 385 nm pulsed excitation, shown as difference spectra (high energy data − low energy data) obtained from a subtraction scaled to the solvent band at 1372 $cm^{-1}$. * indicates a small negative artifact from this subtraction.

of **1**-$Li^+$, -$Na^+$, -$Ca^{2+}$, and -$Ba^{2+}$, providing further evidence that ion release occurs on excitation because redox potentials indicate that the electron transfer needed to form the LLCT state is thermodynamically unfavorable while a metal cation remains bound to the azacrown.[15]

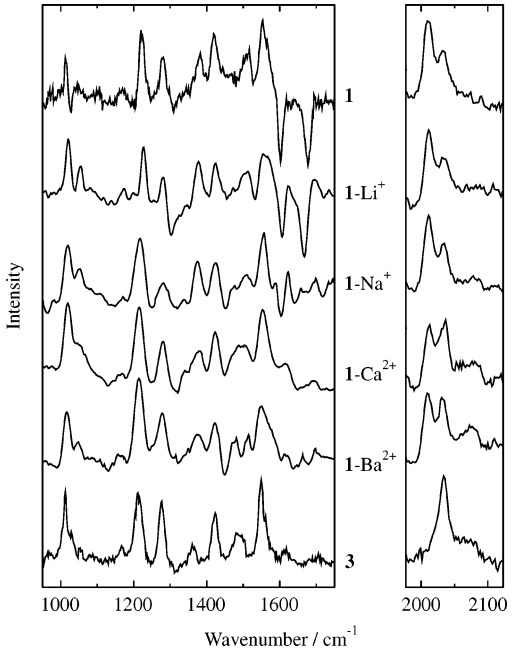


**Figure 6.** Excited state $TR^2$ spectra of **1**-$M^{n+}$ in acetonitrile recorded with 385 nm excitation along with those of **1** and **3**. Shown at 950−1750 $cm^{-1}$ as difference spectra (left; high energy data − low energy data, obtained from a subtraction scaled to the solvent band at 1372 $cm^{-1}$; spectra from **1**-$M^{n+}$ smoothed) and at 1975−2125 $cm^{-1}$ as spectra recorded directly at high energy (right).

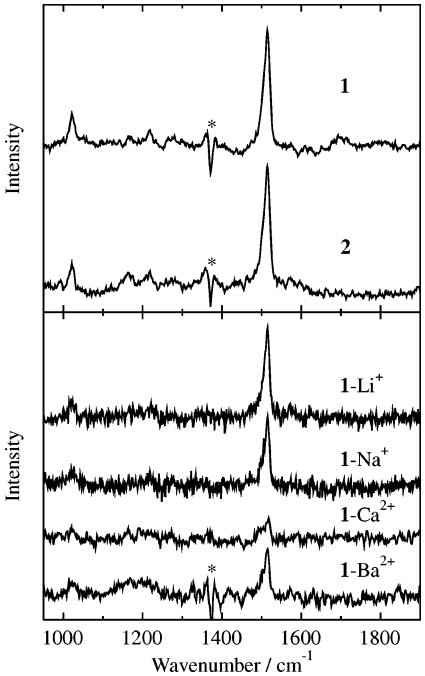


**Figure 7.** Excited state $TR^3$ spectra recorded with 355 nm pumping and 500 nm probing. Top: **1** and **2** in acetonitrile, at a delay time of 8 ns. Bottom: **1**-$M^{n+}$ in acetonitrile, at delay times of 12 ns ($Li^+$), 8 ns ($Na^+$), 25 ns ($Ca^{2+}$), and 20 ns ($Ba^{2+}$). Data shown as difference spectra obtained on subtraction of spectra obtained from the pump only (emission background) and the probe only (solvent and very weak ground-state bands; scaled to the solvent band at 1372 $cm^{-1}$); * indicates a negative artifact from this subtraction.

A second and weaker excited state $\nu(CO)_{Re}$ band at ca. 2080 $cm^{-1}$ is observed from **1**-$M^{n+}$ (Figure 6), and it can be assigned to an MLCT state. The ca. 45 $cm^{-1}$ upshift of this band from its ground state position is characteristic of stronger CO bonds that result from weaker back-bonding because of a decrease in electron density at the oxidized $Re^{II}$ center. Similar upshifts of ca. 40 $cm^{-1}$ have been reported for the equivalent band from time-resolved infrared studies of the MLCT states of other $(bpy)Re(CO)_3L$ complexes, including **4**.[35] The relative intensity of the two excited state $\nu(CO)_{Re}$ bands at ca. 2012 and 2080 $cm^{-1}$ varies with the metal cation (Figure 6), and the observed LLCT:MLCT band intensity ratio decreases in the order $Na^+ \approx Li^+ > Ba^{2+} > Ca^{2+}$.

We have attributed the TRVIS spectra and kinetics observed on 355 nm excitation of these **1**-$M^{n+}$ systems to a combination of MLCT(on), MLCT(off), and LLCT states, with the relative contributions varying with time and depending on the rate of ion release (Scheme 2).[7] All three excited states contain $bpy^{\bullet-}$, which has an absorption band at 370 nm that provides resonance enhancement, and so the relative intensities of the $TR^2$ bands depend on the relative enhancement and on the integrated concentrations of these excited states during the pulse. The MLCT(off) state has the fastest decay rate constant, and the TRVIS analysis indicated that its concentration is low at all times, so any MLCT bands from **1**-$M^{n+}$ may be assigned specifically to the longer-lived MLCT(on) state. Therefore, the observed variation in the relative $\nu(CO)_{Re}$ band intensities with metal cation in the $TR^2$ spectra indicates that the relative LLCT:MLCT(on) state concentration during the pulse decreases in the order $Na^+ \approx Li^+ > Ba^{2+} > Ca^{2+}$. This observation is consistent with the TRVIS analysis, which indicated that the LLCT state is the dominant contributor within <10 ns in the case of fast cation release ($Li^+$, $Na^+$), whereas the MLCT(on) state is dominant in the case of slower release ($Ca^{2+}$, $Ba^{2+}$),[7] and it provides further support for the mechanism in Scheme 2.[7,15]

Overall, the $TR^2$ spectra from **1**-$Li^+$ and -$Na^+$ resemble that from **1**, as characterized particularly by the $\nu(CO)_{Re}$ band and the 1514 $cm^{-1}$ band assigned to the L ligand, and they may be assigned to the LLCT state formed after fast ion release. Outside the $\nu(CO)_{Re}$ region, the $TR^2$ spectrum from **1**-$Ca^{2+}$ resembles that from **3**, as characterized particularly by the broad feature at ca. 1500 $cm^{-1}$ assigned to $\nu_6$ and $\nu_7$ bands of $bpy^{\bullet-}$, and so the bands at <1700 $cm^{-1}$ may be attributed predominantly to the MLCT(on) state of **1**-$Ca^{2+}$, as given in Table 1, consistent with slower ion release. The relatively weak $\nu(CO)_{Re}$ band of the MLCT state observed not only from **1**-$Ca^{2+}$ and **1**-$Ba^{2+}$ but also from **3** and **4**, which form only MLCT excited states, indicates that its RR scattering cross-section is significantly lower than that of the equivalent $\nu(CO)_{Re}$ band of the LLCT state of **1** and **2**.

**Two-Color $TR^3$ Spectra.** $TR^3$ experiments on **1**-**4** were carried out with a pump wavelength of 355 nm and a probe wavelength of 500 nm, which was chosen to provide resonance with a TRVIS band that has been assigned to a transition centered on the phenyl-$NR_2^{\bullet+}$ group of the L ligand in the LLCT state.[16,38] Excited state $TR^3$ bands were not observed on pumping **3** and **4**, and their absence can be attributed to weak resonance enhancement arising from relatively weak transient absorption at this probe wavelength.[16] By contrast, **1** and **2** gave strong and similar $TR^3$ spectra, shown in Figure 7 (top), which are dominated by an intense band at 1514 $cm^{-1}$ and can be attributed to resonance enhancement arising from the strong TRVIS band of the LLCT state.[16]

The ca. 500 nm absorption band of phenyl-dialkylamino radical cations has been assigned to an electronic transition that changes the bonding within the phenyl group and distorts the ring along the axis of the 1,4-substituents, giving strong resonance enhancement to Raman bands arising from modes

that involve motion along this axis.[39] The intense 1514 $cm^{-1}$ $TR^3$ band of **1** and **2** in the LLCT state can be assigned to such a mode involving the Wilson 8a and 9a vibrations of the phenyl ring, downshifted from the equivalent ground state band at ca. 1620 $cm^{-1}$, because of its very strong enhancement in resonance with the electronic transition centered on the phenyl-$NR_2^{\bullet+}$ group. An alternative assignment of this band to a mode involving 8a/9a vibrations within the pyridyl ring, which gives the stronger ground state RR band at 1604 $cm^{-1}$, seems unlikely because it would not be expected to experience such a dominating enhancement in resonance with a phenyl-localized transition. The large downshift in the phenyl 8a/9a band position is characteristic of an increase in the quinoidal character and a decrease in the $\pi$-bonding character of the ring, resulting from oxidation of the donor nitrogen atom and consistent with the canonical structures shown below.[39] A downshift of ca. 40 $cm^{-1}$ in the 8a band has been reported on oxidation to form the radical cation of dimethylaminobenzene[39,40] and the larger downshift of ca. 100 $cm^{-1}$ on forming the LLCT state of **1** and **2** may be due to the electron-withdrawing effect of the para-substituted $Re^{I}$-amidopyridyl group giving a larger decrease in the electron density within the phenyl ring on oxidation, although the shift may also arise, in part, from a change in the form of the mode.

The other $TR^3$ bands observed from the LLCT state of **1** and **2** are relatively weak, occurring at ca. 1370, 1280, 1216, 1165, and 1022 $cm^{-1}$, and they may be assigned to other L-ligand modes. It is likely that these bands arise from vibrations involving the phenyl ring because of resonance enhancement, and that they have undergone shifts from their ground state counterparts that are similar to those reported on formation of other phenyl-dialkylamino radical cations,[38,39] although the forms of the modes may also have changed significantly. Hence, the band at 1216 $cm^{-1}$ may arise from an upshift of the ground-state 9a phenyl vibration at 1184 $cm^{-1}$ and that at 1022 $cm^{-1}$ from a downshift of the ground state mode involving 18b pyridyl and 18a phenyl vibrations at 1030 $cm^{-1}$ (Table 1). Other bands that can be used as diagnostic markers for a change to a more quinoidal structure, such as those arising from $\nu$(phenyl-$NR_2$) and 19a phenyl modes,[40] are not strongly Raman active, and they are not observed in the ground- or excited state Raman spectra of **1** or **2**.

The $TR^3$ spectra obtained from **1**-$M^{n+}$, shown in Figure 7 (bottom), are essentially identical to those obtained from **1** and **2**. They are dominated by the same intense band at 1514 $cm^{-1}$, and so they are assigned similarly to the LLCT state of **1**; again, the observation of LLCT state bands from **1**-$M^{n+}$ samples provides further evidence in support of ion release on excitation, as noted in discussing the $TR^2$ spectra above. The signal-to-noise ratios of the LLCT state bands, from $TR^3$ spectra obtained under comparable conditions, decreased in the order $Li^+ \approx Na^+ > Ba^{2+} > Ca^{2+}$ with the bands from **1**-$Ca^{2+}$ being very weak. This observation indicates that the relative contribution of the LLCT state decreases in this order, and it is consistent with both the $TR^2$ data discussed above and with the TRVIS analysis;[7] the latter indicated that the LLCT state dominates at >10 ns for $Li^+$ and $Na^+$, that there are comparable contributions from LLCT and MLCT(on) states at >30 ns for $Ba^{2+}$, and that the LLCT state is always a minor component for $Ca^{2+}$ because the MLCT(on) state dominates at all times because of its slow rate of ion release.

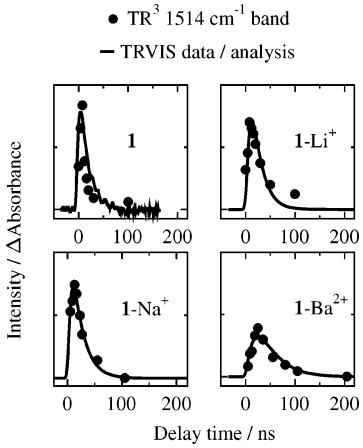


**Figure 8.** Normalized intensity of the $TR^3$ 1514 $cm^{-1}$ band from **1** and **1**-$M^{n+}$ versus delay time along with LLCT state kinetics shown as TRVIS data at 500 nm for **1**, and LLCT components obtained from analysis of TRVIS data at 500 nm according to Scheme 2 for **1**-$M^{n+}$.[7]

The $TR^3$ experiment also enabled the time dependence of the spectra to be monitored, and Figure 8 shows the intensity of the dominant 1514 $cm^{-1}$ band from **1**, **1**-$Li^+$, **1**-$Na^+$, and **1**-$Ba^{2+}$ as a function of delay time,[41] overlaid with the LLCT state kinetics obtained from the TRVIS analysis.[7] Both the rise times and the fall times of the 1514 $cm^{-1}$ $TR^3$ band are longer for **1**-$M^{n+}$ than for **1**, and they depend on the identity of the metal cation, increasing in the order $Na^+ \approx Li^+ < Ba^{2+}$. This trend matches that obtained from the TRVIS analysis of overlapping absorption features,[7] but the clear advantage of the present $TR^3$ experiments is that they have enabled the characteristic vibrational marker bands of the LLCT state to be observed selectively without interference from those of the ground state or the other excited MLCT states. Hence, the $TR^3$ kinetics provide strong and independent evidence in support of the mechanism in Scheme 2.[7]

## Conclusions

We have reported the ground- and excited state Raman spectra of a $[(bpy)Re(CO)_3L]^+$ complex in which L contains an azacrown ether group, along with those of model complexes, using both steady state and time-resolved techniques. Selective resonance enhancement has enabled the vibrations of the L ligand and $Re(CO)_3$(bpy) chromophores and the MLCT and LLCT excited states to be studied selectively.

Single-color $TR^2$ measurements have been used to characterize the excited state structure and bonding in the $(bpy)Re(CO)_3$ group. Model complexes without an electron-donor group showed $bpy^{\bullet-}$ bands indicative of a MLCT excited state, whereas complexes containing an azacrown or dimethylamino donor group showed both $bpy^{\bullet-}$ bands and a downshifted $\nu(CO)_{Re}$ band indicative of a LLCT state. The presence of these LLCT state marker bands from **1**-$M^{n+}$ systems provided evidence that ion release occurs on excitation.

Two-color $TR^3$ measurements have been used to characterize the excited state structure and bonding at the L ligand. The downshift of a phenyl 8a/9a band in the LLCT state is indicative of a change to a more quinoidal structure, and the presence of this LLCT state marker band from **1**-$M^{n+}$ systems has provided further evidence of ion release, along with an independent measure of the LLCT state kinetics.

Together, these Raman studies have provided further evidence to support the photochemical mechanisms given in Schemes 1 and 2, along with more detailed information on structure and

bonding than that available previously from UV−visible spectroscopy.

**Acknowledgment.** We thank L. C. Abbott and A. W. Parker for assistance and helpful discussions and EPSRC for financial support.

**Supporting Information Available:** Characterization details for L**2** and **2**. This material is available free of charge via the Internet at http://pubs.acs.org.

## References and Notes

(1) *Molecular Switches*; Feringa, B. L. Ed.; Wiley-VCH: Weinheim, Germany, 2001.

(2) Adams, S. R.; Kao, J. P. Y.; Grynkiewicz, G.; Minta, A.; Tsien, R. Y. *J. Am. Chem. Soc.* **1988**, *110*, 3212.

(3) Grell, E.; Warmuth, R. *Pure Appl. Chem.* **1993**, *65*, 373.

(4) *Caged compounds*; Marriot, G. Ed.; Methods in Enzymology No. 291; Academic Press: New York, 1998.

(5) Lednev, I. K.; Hester, R. E.; Moore, J. N. *J. Phys. Chem.* **1997**, *101*, 7371.

(6) Lewis, J. D.; Moore, J. N. *Chem. Commun.* **2003**, 2858.

(7) Lewis, J. D.; Perutz, R. N.; Moore, J. N. *J. Phys. Chem. A* **2004**, *108*, 9037.

(8) Plaza, P.; Leray, I.; Changenet-Barret, P.; Martin, M. M.; Valeur, B. *Chem. Phys. Chem.* **2002**, *3*, 668.

(9) Alfimov, M. V.; Fedorova, O. A.; Gromov, S. P. *J. Photochem. Photobiol. A* **2003**, *158*, 183.

(10) Kimura, K.; Sakamoto, H.; Nakamura, M. *Bull. Chem. Soc. Jpn.* **2003**, *76*, 225.

(11) Schanze, K. S.; MacQueen, D. B.; Perkins, T. A.; Cabana, L. A. *Coord. Chem. Rev.* **1993**, *122*, 63.

(12) Vlček, A., Jr.; Busby, M. *Coord. Chem. Rev.* **2006**, *250*, 1755.

(13) Sun, S.-S.; Lees, A. J. *Coord. Chem. Rev.* **2002**, *230*, 171.

(14) Gabrielsson, A.; Hartl, F.; Zhang, H.; Lindsay Smith, J. R.; Towrie, M.; Vlček, A., Jr.; Perutz, R. N. *J. Am. Chem. Soc.* **2006**, *128*, 4253.

(15) MacQueen, D. B.; Schanze, K. S. *J. Am. Chem. Soc.* **1991**, *113*, 6108.

(16) Lewis, J. D.; Bussotti, L.; Foggi, P.; Perutz, R. N.; Moore, J. N. *J. Phys. Chem. A* **2002**, *106*, 12202.

(17) Izatt, R. M.; Pawlak, K.; Bradshaw, J. S.; Bruening, R. L. *Chem. Rev.* **1995**, *95*, 2529.

(18) Schoonover, J. R.; Strouse, G. F. *Chem. Rev.* **1998**, *98*, 1335.

(19) Kalyanasundaram, K. *J. Chem. Soc., Faraday Trans. 2* **1986**, *82*, 2401.

(20) Subsequent IR studies have revealed that a metal cation can bind weakly to the amide carbonyl of the L ligand, as shown by a downshifted amide I band at very high $M^{n+}$ concentrations (e.g., from **2** at $[Ba^{2+}] \geq 0.5$ mol $dm^{-3}$).[21] We did not explore this effect in detail here, but the observed ground state amide I Raman bands show that the azacrown-only bound form was dominant for the $Na^+$, $Ca^{2+}$, and $Ba^{2+}$ samples studied (estimated at ca. >90, 90, and 70%, respectively), with the azacrown-and-amide bound form a minor component; the $Li^+$ sample did not give a distinct second amide I band, but band-fitting indicates that the azacrown-and-amide bound form was more significant.

(21) Lewis, J. D.; Matousek, P.; Towrie, M.; Moore, J. N. Unpublished work.

(22) Lewis, J. D.; Moore, J. N. *Phys. Chem. Chem. Phys.* **2004**, *6*, 4595.

(23) Parker, A. W.; Hester, R. E.; Phillips, D.; Umapathy, S. *J. Chem. Soc., Faraday Trans.* **1992**, *88*, 2649.

(24) Frisch, M. J.; Trucks, G. W.; Schlegel, H. B.; Scuseria, G. E.; Robb, M. A.; Cheeseman, J. R.; Zakrzewski, V. G.; Montgomery Jr., J. A.; Stratmann, R. E.; Burant, J. C.; Dapprich, S.; Millam, J. M.; Daniels, A. D.; Kudin, K. N.; Strain, M. C.; Farkas, O.; Tomasi, J.; Barone, V.; Cossi, M.; Cammi, R.; Mennucci, B.; Pomelli, C.; Adamo, C.; Clifford, S.; Ochterski, J.; Petersson, G. A.; Ayala, P. Y.; Cui, Q.; Morokuma, K.; Malick, D. K.; Rabuck, A. D.; Raghavachari, K.; Foresman, J. B.; Cioslowski, J.; Ortiz, J. V.; Baboul, A. G.; Stefanov, B. B.; Liu, G.; Liashenko, A.; Piskorz, P.; Komaromi, I.; Gomperts, R.; Martin, R. L.; Fox, D. J.; Keith, T.; Al-Laham, M. A.; Peng, C. Y.; Nanayakkara, A.; Gonzalez, C.; Challacombe, M.; Gill, P. M. W.; Johnson, B.; Chen, W.; Wong, M. W.; Andres, J. L.; Gonzalez, C.; Head-Gordon, M.; Replogle, E. S.; Pople, J. A. *Gaussian 98, Revision A.7*; Gaussian, Inc.: Pittsburgh PA, 1998.

(25) Okamoto, H.; Inishi, H.; Nakamura, Y.; Kohtani, S.; Nakagaki, R. *Chem. Phys.* **2000**, *260*, 193.

(26) Rurack, K.; Sczepan, M.; Spieles, M.; Resch-Genger, U.; Rettig, W. *Chem. Phys. Lett.* **2000**, *320*, 87.

(27) Calculated dihedral angles of L**2** at the amide group are: N(H)−C(O)−C(Ph)−C(Ph) 161°; H−N−C−O 171°; C(Py)−N(H)−C(O)−C(Ph) 178°; C(Py)−C(Py)−N(H)−C(O) 176°. For comparison, calculated dihedral angles for the alkene and alkyne diethlyamino analogues[22] are: at the alkene group, C═C−C(Ph)−C(Ph) 176°, C(Py)−C═C−C(Ph) 180°, C(Py)−C(Py)−C═C 178°; and at the alkyne group, C≡C−C(Ph)−C(Ph) 180°, C(Py)−C≡C−C(Ph) 180°, C(Py)−C(Py)−C≡C 180°.

(28) Dollish, F. R.; Fateley, W. G.; Bentley, F. F. *Characeristic Raman Frequencies of Organic Compounds*; John Wiley & Sons, Inc.: New York, 1974.

(29) Tu, A. T. *Raman Spectroscopy in Biology: Principles and Applications*; John Wiley & Sons, Inc.: New York, 1982.

(30) $\nu$(CO) is used to denote stretching of the amide CO group (present in **1**-**3**); $\nu(CO)_{Re}$ is used to denote stretching of the CO ligands attached directly to Re (present in **1**-**4**).

(31) The IR spectra of complexes **1**-**3** show three bands at ca. 1620, 1605, and 1585 $cm^{-1}$ that are observed even more distinctly for the free ligands L**1**−L**3**.[21]

(32) Smothers, W. K.; Wrighton, M. S. *J. Am. Chem. Soc.* **1983**, *105*, 1067.

(33) Gamelin, D. R.; George, M. W.; Glyn, P.; Grevels, F.-W.; Johnson, F. P. A.; Klotzbucher, W.; Morrison, S. L.; Russell, G.; Schaffner, K.; Turner, J. J. *Inorg. Chem.* **1994**, *33*, 3246.

(34) Strommen, D. P.; Mallick, P. K.; Danzer, G. D.; Lumpkin, R. S.; Kincaid, J. R. *J. Phys. Chem.* **1990**, *94*, 1357.

(35) George, M. W.; Johnson, F. P. A.; Westwell, J. R.; Hodges, P. M.; Turner, J. J. *J. Chem. Soc., Dalton Trans.* **1993**, 2977.

(36) Busby, M.; Gabrielsson, A.; Matousek, P.; Towrie, M.; Di Bilio, A. J,; Gray, H. B.; Vlček, A., Jr. *Inorg. Chem.* **2004**, *43*, 4994.

(37) Bradley, P. G.; Kress, N.; Hornberger, B. A.; Dallinger, R. F.; Woodruff, W. H. *J. Am. Chem. Soc.* **1981**, *103*, 7441.

(38) Hester, R. E.; Williams, K. P. J. *J. Chem. Soc., Perkin Trans. 2* **1982**, 559.

(39) Poizat, O.; Guichard, V.; Buntinx, G. *J. Chem. Phys.* **1989**, *90*, 4697.

(40) Brouwer, A. M.; Wilbrandt, R. *J. Phys. Chem.* **1996**, *100*, 9678.

(41) The $TR^3$ signal from **1**-$Ca^{2+}$ was too weak for kinetic measurements.